A novel rotifer-derived alkaloid paralyzes schistosome larvae and prevents infection

Jiarong Gao[1,2,9], Ning Yang[3,9], Fred A. Lewis[4^], Peter Yau[5], James J. Collins III[2†], Jonathan V. Sweedler[3*], Phillip A. Newmark[2,6,7,8*]

[1]Cellular and Molecular Biology Program, University of Wisconsin-Madison, Madison, WI, USA. [2]Department of Cell and Developmental Biology, University of Illinois at Urbana-Champaign, Urbana, IL, USA. [3]Department of Chemistry, University of Illinois at Urbana-Champaign, Urbana, IL, USA. [4]Biomedical Research Institute, Rockville, MD, USA. [5]Roy J. Carver Biotechnology Center, University of Illinois at Urbana-Champaign, Urbana, IL, USA. [6]Howard Hughes Medical Institute, USA. [7]Morgridge Institute for Research, Madison, WI, USA. [8]Department of Integrative Biology, University of Wisconsin-Madison, Madison, WI, USA. [9]These authors contributed equally: Jiarong Gao, Ning Yang.

[*]e-mail: jsweedle@illinois.edu; pnewmark@morgridge.org

[^]Present address: Bernville, PA, USA

[†]Present Address: Department of Pharmacology, UT Southwestern Medical Center, Dallas, TX, USA

Schistosomiasis, caused by the blood fluke *Schistosoma*, is a devastating and widespread disease affecting more than 200 million people and threatening over 700 million people worldwide[1,2]. Treatment relies exclusively on one drug, praziquantel, for which there are concerns of emerging drug resistance[3,4] and which has shown some limitations in mass drug administration programs[5]. Efforts to develop an effective vaccine to combat schistosomiasis have been unsuccessful; thus, there is an urgent need for alternative drugs and better prevention strategies. Here we report the discovery and purification of a novel tetracyclic alkaloid secreted by the rotifer *Rotaria rotatoria,* which lives commensally on snails that serve as intermediate hosts for *S. mansoni*[6]. This compound effectively paralyzes cercariae, the infective larvae of schistosomes, at nanomolar concentrations. Furthermore, we show that worm burden and disease pathology are significantly reduced when cercariae are pre-treated with this Schistosome Paralysis Factor (SPF). Identifying this molecule provides new directions for understanding motility of schistosome cercariae and new strategies for preventing schistosomiasis.

Schistosomes have a complex life cycle that alternates between an intermediate host (snail) and a definitive host (mammal) via two free-living, water-borne forms called miracidia and cercariae, respectively[7] (Fig. 1a). For decades, inconsistency in cercarial production by snails and infectivity of mammalian hosts has been observed in most schistosome laboratories[8]. Intriguingly, Stirewalt and Lewis reported that rotifer colonization on snail (*Biomphalaria glabrata*) shells significantly reduced cercariae output, motility, and infectivity[6]. Furthermore, they observed that cercarial motility was affected not only by the presence of rotifers, but also by rotifer-conditioned water,

42 indicating that rotifers released water-soluble molecules with paralytic activity. Almost
43 40 years have passed since this important finding, yet this factor's identity has remained
44 a mystery.

45 Encouraged by this anti-cercarial effect and its potential to prevent schistosome
46 infection, we sought to purify this paralyzing agent. We isolated individual rotifers from
47 snail shells and found two species, *Rotaria rotatoria* (Fig. 1b) and *Philodina acuticornis*
48 (Fig. 1c), as previously reported[6]. To identify which rotifer was responsible for the
49 paralytic effect, we grew clonal isolates of each species, producing rotifer-conditioned
50 artificial pond water (APW). Adding *Rotaria*-conditioned APW to freshly collected
51 cercariae resulted in gradual paralysis within five minutes (Fig. 1d). Most cercariae
52 stopped swimming and sank to the bottom of the dish. Tapping the dish could stimulate
53 their movement, but their response was limited to writhing on the dish bottom or short-
54 distance swimming before becoming paralyzed again. In contrast, *P. acuticornis*-
55 conditioned water had no effect (Fig. 1e).

56 To purify the paralyzing agent, we performed molecular weight cut-off filtration (MWCO)
57 of rotifer-conditioned water and found that the activity was present in the <650 Da
58 fraction. The <650 Da filtrate was fractionated by reversed-phase high-performance
59 liquid chromatography (RP-HPLC) (Fig 2a) and each fraction was tested on cercariae.
60 Paralysis was only observed following treatment with a peak eluting at 25-27 min (Fig.
61 2b). As expected, this peak was detected only in *R. rotatoria*- but not *P. acuticornis*-
62 conditioned water (Fig. 2b). A second round of HPLC on this peak revealed one peak
63 (eluting at 24-26 min) with paralytic activity (Fig. 2c). A predominant signal of 273.16 Da
64 (M+H) in this peak was revealed by matrix-assisted laser desorption/ionization mass

65 spectrometry (MALDI-MS) (Fig. 2d). Consistent with the paralysis assay, this signal (m/z
66 273.16) was detected exclusively in the fraction eluting at 24-26 min but not in the
67 fractions before or after (Fig. 2e). These results suggested that the component with m/z
68 273.16 was the paralyzing agent, which we named "Schistosome Paralysis Factor"
69 (SPF). We then determined the monoisotopic mass for protonated SPF using high-
70 resolution quadrupole time-of-flight (Q-TOF) MS, 273.1595 Da (Fig. 2f), suggesting
71 $C_{16}H_{20}N_2O_2$ as the best-fitting formula for SPF.

72 To elucidate its structure, we purified SPF from *R. rotatoria*-conditioned water, obtaining
73 0.126 mg from 25 L. Nuclear magnetic resonance (NMR) spectroscopy revealed a novel
74 tetracyclic structure, which conformed to the best-fitting formula and contained one
75 exchangeable proton, consistent with the results of H/D-exchange MS (Fig. 2g;
76 Extended Data Fig. 1-6; Extended Data Table 1). Nuclear Overhauser effect
77 spectroscopy (NOESY) (Extended Data Fig. 7) and 3D minimized steric-energy models
78 favored the (R, S, S) configuration (steric energy 35.6 kcal/mol) over the (S, R, R)
79 configuration (110.9 kcal/mol) at the three chiral centers, C12-14. Based on energy-
80 minimized models, the proton-proton spatial distance in the (R, S, S) configuration
81 matched the relative intensity of cross-peak signals in NOESY, whereas the distances
82 in the (S, R, R) configuration did not (Extended Data Table 2; Extended Data Fig. 7).

83 To test its dose dependency, we examined the paralytic effect of serially diluted SPF on
84 cercariae by quantifying their movement over time. In the absence of SPF, over 82% of
85 cercariae were free-swimming over three minutes (Fig. 3a). In 2.5 nM SPF, the
86 percentage of free-swimming cercariae dropped to 67% at three-minutes post drug
87 treatment. As the concentration of SPF increased, so did the rate of paralysis, and more

88 cercariae were paralyzed at the end of treatment. We observed maximum effects in 250
89 nM and 2.5 μM SPF, with the majority of cercariae paralyzed within 30 s.

90 Two natural compounds isolated from *Streptomyces sp.*, ht-13-A and ht-13-B[9], are
91 structurally related to SPF. All three alkaloids share a novel oxepineindole framework
92 fused with a pyrrolidine ring (Fig. 3a-c). Although synthesis of SPF has not been
93 achieved, total syntheses of ht-13-A and ht-13-B have been reported[10-12]. To test
94 whether this shared tetracyclic scaffold is responsible for the paralytic effect, we
95 analyzed structure-activity relationships by using ht-13-A, ht-13-B, three ht-13-A
96 derivatives, and one epimer in cercarial paralysis assays. Importantly, ht-13-A, although
97 not as potent as SPF, also had a paralytic effect on cercariae (Fig. 3b). In contrast, ht-
98 13-B did not paralyze cercariae, suggesting that the extra methyl group disrupts
99 interaction with the target (Fig. 3c). Of the three ht-13-A analogs, only ht-13-A-pr
100 effectively paralyzed cercariae; it was more potent than ht-13-A, indicating that the
101 nature of the side chain is important for proper target interaction (Fig. 3d-e). In contrast
102 to ht-13-A, the epimer was unable to paralyze cercariae, supporting the (R, S)
103 configuration of SPF at C12, 13.

104 Since motility of the cercarial tail is essential for swimming and provides force for skin
105 penetration[13-15], we examined whether SPF prevented infection. We treated ~200
106 cercariae with different concentrations of SPF for 10 mins, and tested their ability to
107 infect mice after a 30-min exposure to their tails (N=6 for each condition). Six-weeks
108 post infection, we euthanized the mice, counted schistosomes recovered after hepatic
109 portal vein perfusion, and examined liver pathology. From controls, we recovered 83
110 adult worms on average (Fig. 4a), consistent with typical recoveries of ~40%[16]. Livers

111 from these mice appeared dark and contained extensive granulomas (Fig. 4a). In
112 contrast, we did not recover any adult worms from mice after treatment with 250 nM or
113 2.5 μM SPF (Fig. 4b) and no granulomas were observed (Fig. 4a). Histological
114 examination confirmed that these livers were free of schistosome eggs (Fig. 4e),
115 suggesting complete inhibition of infection. These data are consistent with the full
116 paralysis observed after treatment with 250 nM or 2.5 μM SPF (Fig. 3a). Although 25
117 nM SPF paralyzed most cercariae *in vitro*, the effects on mouse infection were not as
118 severe (Fig. 4a). Mechanical and/or chemical stimuli from mouse tails may overcome
119 SPF-induced paralytic effects at low SPF concentrations. Notably, neither Ht-13-A nor
120 Ht-13-A-pr blocked infection as completely as 250 nM SPF, even at 25 μM (Fig. 4a, c, d,
121 f, g). Under more realistic infection conditions, in which mouse tails were lifted 1-2 cm
122 from the bottom of the test tube containing cercariae, so they had to swim actively
123 towards the tail to infect the mouse, Ht-13-A and Ht-13-A-pr were still not as effective as
124 SPF, which completely blocked infection (Extended Data Fig. 8).

125 This work has identified a novel tetracyclic alkaloid, produced by the rotifer *R. rotatoria,*
126 that paralyzes the infective larvae of schistosomes. Although its mechanism of action
127 remains unknown, its chemical structure provides important clues. SPF contains a
128 serotonin backbone, suggesting that SPF might antagonize serotonin signaling, perhaps
129 via G protein-coupled receptors (GPCRs) or serotonin-gated channels. Consistent with
130 this idea, the structurally related compounds, ht-13-A and ht-13-B, bind several human
131 serotonin receptors[9]. In schistosomes, serotonin has been implicated in neuromuscular
132 functions in multiple life stages[17-20]; knocking down a serotonergic GPCR (Sm5HTR) in
133 schistosomulae and adult worms led to decreased movement[21]. Interestingly,

134 praziquantel partially activates human HT2BR, suggesting that it may also target
135 schistosome serotonergic GPCRs[22].

136 The chemical ecology underlying *R. rotatoria*'s production of SPF is also unclear.
137 Whether SPF is used naturally to combat other aquatic creatures (e.g., to prevent other
138 rotifers from colonizing areas where *R. rotaria* live) and, thus, the effect on schistosome
139 cercariae is indirect, or whether SPF benefits the rotifer's commensal host will require
140 further study. In the past few decades, the discovery and development of natural
141 products have helped combat parasitic diseases[23]. Based on its ability to block infection,
142 SPF holds great promise as an anti-schistosomal agent. Identifying the biologically
143 active chemical scaffolds and understanding SPF's mode of action are expected to
144 provide important clues for preventing schistosomiasis.

145 **Methods**

146 **Artificial pond water**

147 Four stock solutions were prepared to make artificial pond water[24]: 1) 0.25 g/L $FeCl_3 \cdot$
148 $6H_2O$, 2) 12.9 g/L $CaCl_2 \cdot 2H_2O$, 3) 10g/L $MgSO_4 \cdot 7H_2O$, and 4) 34 g/L KH_2PO_4 1.5 g/L
149 $(NH_4)_2SO_4$, pH 7.2. For 1L artificial pond water, we added 0.5 mL of $FeCl_3$ solution, 2.5
150 mL $CaCl_2$ solution, 2.5 mL $MgSO_4$ solution and 1.25 mL phosphate buffer.

151 **Obtaining *S. mansoni* cercariae**

152 Infected *B. glabrata* snails provided by Biomedical Research Institute (BRI, Rockville,
153 MD) were maintained in artificial pond water and fed Layer Crumbles (chicken feed)
154 (Rural King, Mattoon, IL). To obtain *S. mansoni* cercariae, *B. glabrata* snails were
155 exposed to light at 26°C for 1-2 hrs. Artificial pond water containing cercariae was
156 passed through 100 μm cell strainer (Falcon) to remove snail food and feces. Cercariae
157 were then collected using custom-made 20 μm cell strainers.

158 **Rotifer culture**

159 Since both rotifer species reproduce parthenogenetically, we clonally expanded each
160 species into one-liter cultures from a single rotifer. Individual rotifers (*R. rotatoria* and *P.*
161 *acuticornis*) were initially isolated from the shell of *B. glabrata* and cultured in artificial
162 pond water in 24-well plates. Each individual colony was expanded into ever-larger
163 culture volumes and ultimately maintained in two-liter flasks. Both species were fed
164 Roti-rich liquid invertebrate food (Florida Aqua Farms Inc). Rotifer-conditioned water
165 was collected every month by filtering out the rotifers using a 20 μm cell strainer.

166 Filtered rotifers were then passaged to fresh artificial pond water to propagate the
167 cultures.

168 **Crude rotifer-conditioned water preparation**

169 One liter rotifer media was lyophilized, reconstituted with 50 mL dH_2O and filtered
170 through 10,000 and 650 (MWCO) Pall Minimate TFF Capsules with Omega membrane
171 (Ann Arbor, MI). Filtrate (<650 Da) was freeze dried. For RP-HPLC, 300 mg of the dried
172 material was dissolved in dH_2O and run on a RP-HPLC – Merck Chromolith semi-prep
173 RP-18e column (Darmstadt, Germany) at 5 ml/min using a gradient of 100% A to 60% B
174 in 60 min. 10 mL fractions were collected and assayed for biological activity. Fractions
175 containing biological activity were saved for further study.

176 **Further purification of rotifer media**

177 The bioactive fractions were pooled, freeze dried with SpeedVac (Savant, MA),
178 reconstituted with 500 μL dH_2O and injected into a 4.6mm diameter × 25cm Symmetry
179 column (Waters, MA). Breeze2 analytical LC system (Waters, MA) was employed for
180 separation at 0.5 ml/min with the following solvents and gradients: Solvent A, 0.1%
181 formic acid (FA); solvent B, methanol with 0.1% FA; 0—10 min 0—10% B, 10—30 min
182 10—35% B, 30—33 min 35—80% B, 33—37 min 80—80% B, 37—40 min 80—0% B.
183 Eluents were collected manually based on peak elution. All fractions were lyophilized,
184 reconstituted with water and analyzed with MALDI-MS. Fractions containing biological
185 activity were saved for future use.

186 **Matrix-assisted laser desorption/ionization mass spectrometry (MALDI-MS)**
187 **analysis**
188 For each collected fraction, 1 μL of sample solution was spotted on ground steel MALDI
189 target and mixed with 1 μL of alpha-cyano-4-hydroxy-cinnamic acid (CHCA, Sigma-
190 Aldrich, MO) solution (10 mg/mL CHCA in 50% acetonitrile solution with 0.005%
191 trifluoroacetic acid). Mass calibration, spectra acquisition and analysis were performed
192 under conditions as previously described[25].

193 **High-resolution quadrupole time-of-flight mass spectrometry (Q-TOF MS)**
194 **analysis**
195 1 μL of the bioactive fraction was separated on a Magic 0.1 × 150mm column (Michrom,
196 CA) and analyzed with maXis 4G mass spectrometer (Bruker, MA) using previously
197 established methods for metabolite study[26]. The separation was performed at 300
198 nl/min by use of solvent A (95% water, 5% acetonitrile with 0.1% FA) and solvent B (5%
199 water, 95% acetonitrile with 0.1% FA) with the following gradient conditions: 0—5 min
200 4% B, 5—50 min 4—50% B, 50—52 min 50—90% B, 52—60 min 90% B, 60—70 min
201 90—4% B, 70—90 min 4% B.

202 **Hydrogen/deuterium (H/D) exchange analysis**
203 Acidified deuterated methanol (CD_3OD, methanol—d4, Sigma—Aldrich, MO) was made
204 by adding 1 μL of deuterated FA into 1 mL of CD_3OD. 2 μL of the bioactive fractions
205 were added into 18 μL of acidified methanol above. 15 μL of the mixture were analyzed
206 by direct infusion into a modified 11 Tesla FTMS (Thermo Scientific, MA) through
207 NanoMate robot (Advion, NY)[27]. Full spectra were acquired with resolution set at 100k.

208 **Nuclear magnetic resonance (NMR) analysis**

209 Purified bioactive materials were dissolved in 250 µL of CD_3OD and transferred into a 5
210 mm Shigemi NMR tube with a glass magnetic plug with susceptibility matched to
211 CD_3OD on the bottom. All NMR data were collected at 40°C on an Agilent VNMRS 750
212 MHz spectrometer equipped with a 5 mm Varian indirect detection probe with z gradient
213 capability. Collected NMR data included 1H spectrum, gradient selected correlation
214 spectroscopy (gCOSY), total correlation spectroscopy (TOSCY), nuclear overhauser
215 enhancement spectroscopy (NOESY) with a mixing time of 500 ms, heteronuclear
216 single quantum coherence spectroscopy (^{1}H—^{13}C HSQC) and heteronuclear multiple-
217 bond correlation spectroscopy (^{1}H—^{13}C HMBC). The NMR spectra were analyzed using
218 Mnova NMR software (Mestrelab Research, Spain).

219 **Determination of SPF concentration**

220 The proton quantification experiments were performed at 23°C on an Agilent 750 MHz
221 VNMRS NMR spectrometer equipped with a 5mm triple-resonance (^{1}H/^{13}C/^{15}N) indirect-
222 detection probe with XYZ PFG gradient capability. The probe was calibrated using the
223 qEstimate tool in the Agilent VnmrJ4.2 software with a known standard. The proton
224 spectrum of the sample was collected with a 90-degree pulse angle of 8.5 ms, 16 scans
225 and 10.4 s delay between scans. The Agilent VnmrJ4.2 software was used to determine
226 the concentration of the sample based on the integration values of proton peaks. A total
227 of 5 well-resolved proton peaks (7.12ppm (1H), ~6.89ppm (2H), 4.41 (1H), 3.83 (3H),
228 and ~3.58 (2H)) was used, and the concentration of the sample was 1.55 ± 0.07 mM. All
229 concentrations used in the cercarial paralysis assay were calculated based on this
230 value.

231 **Cercarial paralysis assay**

232 To capture the whole field while avoiding excess reflected light in a well, we used the lid
233 of 96-well plate (Costar). 40 μL of artificial pond water containing ~50 cercariae were
234 added to each shallow well on the lid. 10 μL of SPF (dissolved in APW) was then added
235 to reach the final concentration indicated. Using a high-speed camera (Olympus i-
236 SPEED TR), attached to a stereomicroscope (Leica MZ125), we recorded cercariae
237 movement at 20-60 fps at 1.25X magnification just prior to addition of test compounds
238 until 3-4 min after treatment started. Raw movies were converted to .avi files using i-
239 SPEED Viewer and compressed into JPEG format using ImageJ (addition of compound
240 is considered time 0). We then counted the numbers of free swimming/paralyzed
241 cercariae every 5 s for 1 min and every 30 s thereafter for 3 min. The number of dead
242 cercariae (those that never swim before and after SPF treatment) were subtracted from
243 data. Experiments were performed in biological triplicate.

244 **Mouse infectivity assay**

245 Mouse infections were performed by exposing mouse tails to *S. mansoni* cercariae
246 according to standard protocol from BRI[16] with slight modifications. Briefly, we secured
247 mice in rodent restrainers (Thomas Scientific, Cat #551-BSRR) and put them vertically
248 on top of a rack with grids. We pipetted 100 μL of each drug at proper concentration into
249 a skinny glass tube (Fisher Scientific, Cat #14-958A) inside a 12 X 75 mm holding glass
250 tube (VWR, Cat # 47729-570). 300 μL of APW containing ~200 cercariae were pipetted
251 into each skinny tube and incubated for 10 mins before we inserted the mouse tail.
252 Mouse tails were wiped with APW-moistened Kimwipes, inserted into the skinny tube,
253 and exposed to cercariae for 30 mins. The mouse tail was touching the bottom of the

254 test tube unless otherwise specified. We euthanized and perfused these mice six week-
255 post infection according to standard protocols[16]. For each drug, we initially used three
256 mice for controls (APW only) and three mice for each concentration tested except for 25
257 nM Ht-13-A and Ht-13-A-pr. We then repeated the experiments again with three mice
258 for each condition. In addition to that, we included six mice for 25 nM Ht-13-A and Ht-
259 13-A-pr.

260 Adult worms were recovered by hepatic portal vein perfusion and briefly incubated in
261 2.5% Tricaine (Sigma) to separate males and females. We counted total numbers of
262 adult worms under a stereomicroscope (Leica MZ75). Livers from infected mice were
263 fixed in 4% formaldehyde in PBS overnight. Largest liver lobes (left lobe) were
264 submitted to University of Wisconsin-Madison Histology Core Facility for sectioning and
265 Hematoxylin and Eosin staining. Each left lobe was evenly cut into 4-6 pieces and
266 paraffin embedded on a large cassette. One slide (4-6 liver sections) for each liver was
267 used for histological examination, which provided a representative view throughout the
268 whole liver lobe. We took a tiled image of the whole slide using a Zeiss Axio Zoom
269 microscope and used ImageJ to determine the area of each section. Total numbers of
270 eggs in each section were counted and normalized to the area.

271 In adherence to the Animal Welfare Act and the Public Health Service Policy on
272 Humane Care and Use of Laboratory Animals, all experiments with and care of mice
273 were performed in accordance with protocols approved by the Institutional Animal Care
274 and Use Committee (IACUC) of the University of Wisconsin-Madison (protocol approval
275 number M005569).

276 **Statistical analysis**

277 GraphPad Prism (Version 7) was used for all statistical analyses. One-way ANOVA test
278 followed by Dunnett's multiple comparison test was used. Mean ± S.D. is shown in all
279 figures.

280 1 Steinmann, P., Keiser, J., Bos, R., Tanner, M. & Utzinger, J. Schistosomiasis and water
281 resources development: systematic review, meta-analysis, and estimates of people at
282 risk. *The Lancet. Infectious diseases* **6**, 411-425, doi:10.1016/S1473-3099(06)70521-7
283 (2006).
284 2 WHO. Schistosomiasis and soil-transmitted helminthiases: number of people treated in
285 2016. *Wkly Epidemiol Rec* **92**, 749-760 (2017).
286 3 Doenhoff, M. J., Cioli, D. & Utzinger, J. Praziquantel: mechanisms of action, resistance
287 and new derivatives for schistosomiasis. *Current opinion in infectious diseases* **21**, 659-
288 667, doi:10.1097/QCO.0b013e328318978f (2008).
289 4 Wang, W., Wang, L. & Liang, Y. S. Susceptibility or resistance of praziquantel in human
290 schistosomiasis: a review. *Parasitol Res* **111**, 1871-1877, doi:10.1007/s00436-012-3151-z
291 (2012).
292 5 Assare, R. K. *et al.* Sustaining Control of Schistosomiasis Mansoni in Western Cote
293 d'Ivoire: Results from a SCORE Study, One Year after Initial Praziquantel Administration.
294 *PLoS Negl Trop Dis* **10**, e0004329, doi:10.1371/journal.pntd.0004329 (2016).
295 6 Stirewalt, M. & Lewis, F. A. Schistosoma mansoni: effect of rotifers on cercarial output,
296 motility and infectivity. *Int J Parasitol* **11**, 301-308 (1981).
297 7 Basch, P. F. Schistosomes : development, reproduction, and host relations. *New York :*
298 *Oxford University Press*, 248 p (1991).
299 8 Lewis, F. A., Stirewalt, M. A., Souza, C. P. & Gazzinelli, G. Large-scale laboratory
300 maintenance of Schistosoma mansoni, with observations on three schistosome/snail
301 host combinations. *J Parasitol* **72**, 813-829 (1986).
302 9 Kamigauchi, T. & Yasui, M. Heterocyclic compounds having affinities for serotonin
303 receptors. WO/2000/059909 (2000).
304 10 Zhang, Y. L., McArdle, I. W., Hubbard, J. W., Akhmedov, N. G. & Soderberg, B. C. G. Total
305 synthesis of the tetracyclic indole alkaloid ht-13-A. *Tetrahedron Lett* **57**, 2865-2867,
306 doi:10.1016/j.tetlet.2016.05.060 (2016).
307 11 Tao, P., Chen, Z. & Jia, Y. A concise gram-scale synthesis of ht-13-A via a rhodium-
308 catalyzed intramolecular C-H activation reaction. *Chem Commun (Camb)* **52**, 11300-
309 11303, doi:10.1039/c6cc05930a (2016).
310 12 Zhang, Y., Hubbard, J. W., Akhmedov, N. G., Petersen, J. L. & Soderberg, B. C. Total
311 synthesis of the tetracyclic indole alkaloid ht-13-B. *J Org Chem* **80**, 4783-4790,
312 doi:10.1021/acs.joc.5b00433 (2015).
313 13 Haas, W. Physiological analysis of cercarial behavior. *J Parasitol* **78**, 243-255 (1992).
314 14 Haas, W. Parasitic worms: strategies of host finding, recognition and invasion. *Zoology*
315 *(Jena)* **106**, 349-364, doi:10.1078/0944-2006-00125 (2003).
316 15 Whitfield, P. J., Bartlett, A., Khammo, N. & Clothier, R. H. Age-dependent survival and
317 infectivity of Schistosoma mansoni cercariae. *Parasitology* **127**, 29-35 (2003).
318 16 Lewis, F. Schistosomiasis. *Curr Protoc Immunol* **Chapter 19**, Unit 19 11,
319 doi:10.1002/0471142735.im1901s28 (2001).
320 17 Ribeiro, P., Gupta, V. & El-Sakkary, N. Biogenic amines and the control of neuromuscular
321 signaling in schistosomes. *Invertebrate neuroscience : IN* **12**, 13-28, doi:10.1007/s10158-
322 012-0132-y (2012).

323 18 Boyle, J. P., Zaide, J. V. & Yoshino, T. P. Schistosoma mansoni: effects of serotonin and
324 serotonin receptor antagonists on motility and length of primary sporocysts in vitro. *Exp*
325 *Parasitol* **94**, 217-226, doi:10.1006/expr.2000.4500 (2000).
326 19 Boyle, J. P. & Yoshino, T. P. Serotonin-induced muscular activity in Schistosoma mansoni
327 larval stages: importance of 5-HT transport and role in daughter sporocyst production. *J*
328 *Parasitol* **91**, 542-550, doi:10.1645/GE-432R (2005).
329 20 Chan, J. D. *et al.* A Miniaturized Screen of a Schistosoma mansoni Serotonergic G
330 Protein-Coupled Receptor Identifies Novel Classes of Parasite-Selective Inhibitors. *PLoS*
331 *Pathog* **12**, e1005651, doi:10.1371/journal.ppat.1005651 (2016).
332 21 Patocka, N., Sharma, N., Rashid, M. & Ribeiro, P. Serotonin signaling in Schistosoma
333 mansoni: a serotonin-activated G protein-coupled receptor controls parasite movement.
334 *PLoS Pathog* **10**, e1003878, doi:10.1371/journal.ppat.1003878 (2014).
335 22 Chan, J. D. *et al.* The anthelmintic praziquantel is a human serotoninergic G-protein-
336 coupled receptor ligand. *Nat Commun* **8**, 1910, doi:10.1038/s41467-017-02084-0 (2017).
337 23 Shen, B. A New Golden Age of Natural Products Drug Discovery. *Cell* **163**, 1297-1300,
338 doi:10.1016/j.cell.2015.11.031 (2015).
339 24 Collins, J. J., 3rd, King, R. S., Cogswell, A., Williams, D. L. & Newmark, P. A. An atlas for
340 Schistosoma mansoni organs and life-cycle stages using cell type-specific markers and
341 confocal microscopy. *PLoS Negl Trop Dis* **5**, e1009, doi:10.1371/journal.pntd.0001009
342 (2011).
343 25 Tillmaand, E. G. *et al.* Peptidomics and Secretomics of the Mammalian Peripheral
344 Sensory-Motor System. *J Am Soc Mass Spectrom* **26**, 2051-2061, doi:10.1007/s13361-
345 015-1256-1 (2015).
346 26 Aerts, J. T. *et al.* Patch clamp electrophysiology and capillary electrophoresis-mass
347 spectrometry metabolomics for single cell characterization. *Anal Chem* **86**, 3203-3208,
348 doi:10.1021/ac500168d (2014).
349 27 Lee, J. E. *et al.* Endogenous peptide discovery of the rat circadian clock: a focused study
350 of the suprachiasmatic nucleus by ultrahigh performance tandem mass spectrometry.
351 *Mol Cell Proteomics* **9**, 285-297, doi:10.1074/mcp.M900362-MCP200 (2010).
352 28 Collins, J. J., 3rd & Newmark, P. A. It's no fluke: the planarian as a model for
353 understanding schistosomes. *PLoS Pathog* **9**, e1003396,
354 doi:10.1371/journal.ppat.1003396 (2013).
355

356 **Acknowledgements**

357 *B. glabrata* snails were provided by the NIAID Schistosomiasis Resource Center of the
358 Biomedical Research Institute (Rockville, MD) through NIH-NIAID Contract
359 HHSN272201700014I for distribution through BEI Resources. We thank: Melanie
360 Issigonis, Umair Khan, Jayhun Lee, and Tania Rozario for helpful comments on the
361 manuscript; Tracy Chong and Jayhun Lee for help maintaining the schistosome life
362 cycle; Björn Söderberg and Yanxing Jia for providing Ht-13-A, -B, and derivatives;
363 Lingyang Zhu for expert assistance with NMR; Brian Imai for assistance with SPF
364 purification; as well as Peg Stirewalt, James Leef, Tom Nerad, and Paul Mazzocchi for
365 their early efforts to help solve this puzzle. This work was supported by the National
366 Institutes of Health P30 DA018310 and R01 NS031609 to JVS. JG was supported by an
367 HHMI International Student Research Fellowship. PAN is an investigator of Howard
368 Hughes Medical Institute. The content is solely the responsibility of the authors and
369 does not necessarily represent the official views of the National Institutes of Health.

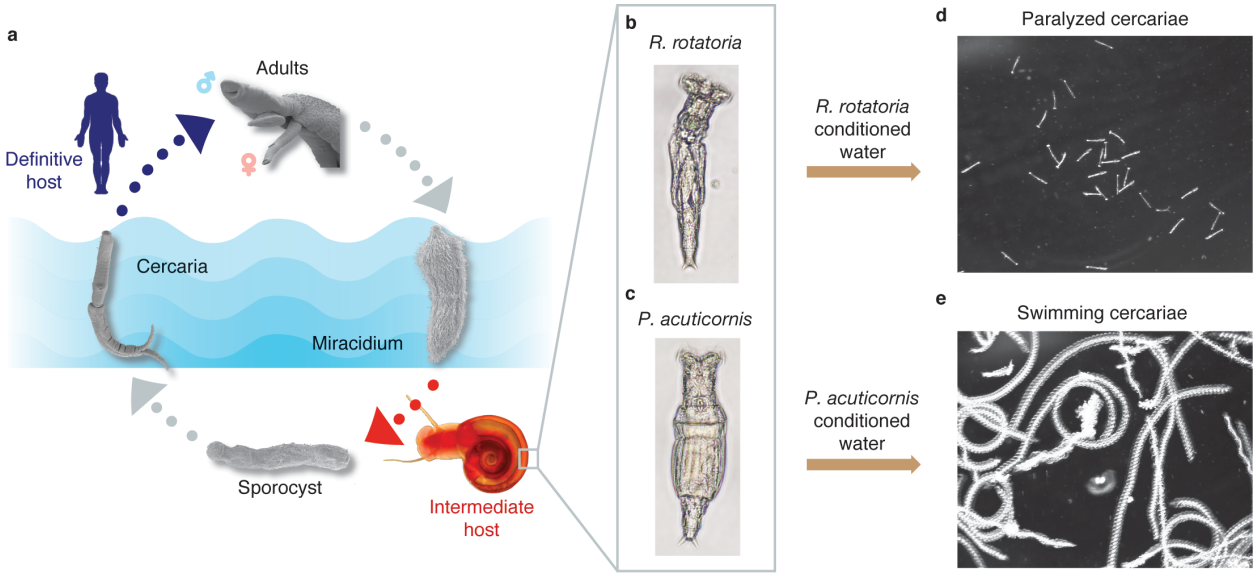

Figure 1 | *R. rotatoria*-conditioned water paralyzes *S. mansoni* cercariae. a, Life cycle of *S. mansoni* adapted from [28]. **b,c,** Bright-field microscopy images of *R. rotatoria* and *P. acuticornis*. **d, e,** Maximum intensity projection (5 s, 150 frames) of cercariae motility after treatment with *R. rotatoria*- or *P. acuticornis*- conditioned water.

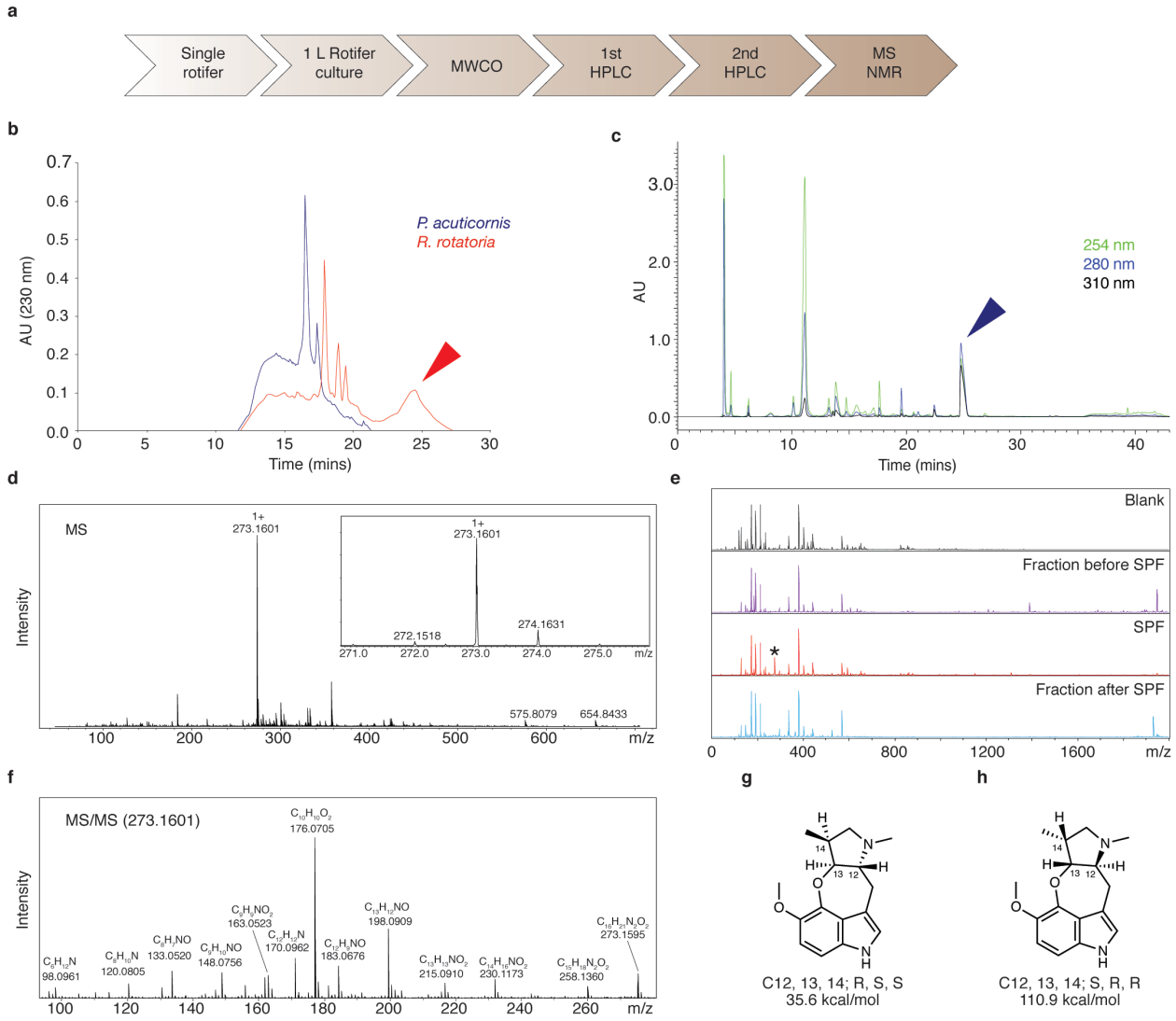

Figure 2 | SPF is a novel tetracyclic alkaloid. a, Flowchart for SPF purification. **b,** 1st HPLC plots of *R. rotatoria*- and *P. acuticornis*-conditioned water. Red arrowhead indicates the peak containing bioactivity. **c,** 2nd HPLC plot of the bioactive fraction (red arrowhead in **b**). Blue arrowhead indicates the peak containing bioactivity. **d,** MS showing the dominant signal of m/z 273.1601 from the peak (blue arrowhead). **e,** MS plots showing this signal (asterisk, m/z 273.1601) was only detected in the fraction eluting at 24-26 min. **f,** Tandem MS acquired from high-resolution Q-TOF analysis. **g, h,** NOESY resolved the relative stereochemistry of three chiral centers and narrowed it down to two possible configurations. Predicted steric energy for the R,S,S (**g**) and S,R,R (**h**) stereoisomers is shown.

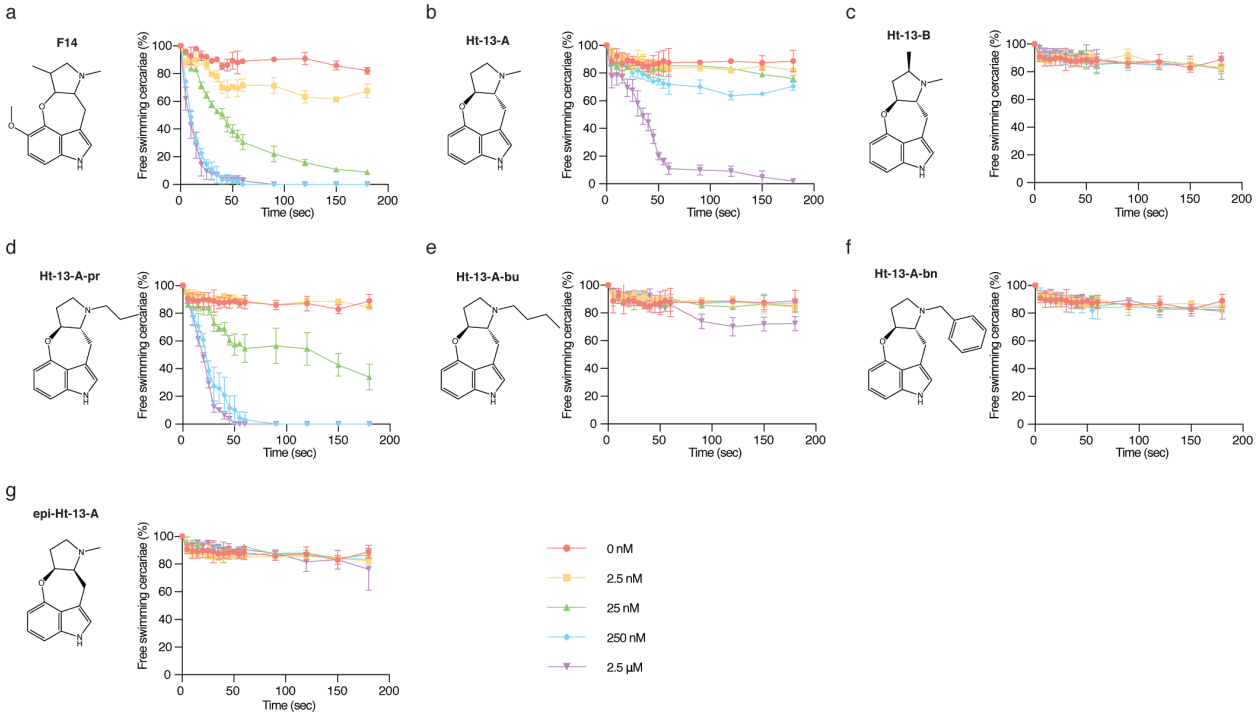

Figure 3 | Structure-activity relationships of SPF and related compounds as measured by cercarial motility assays. a-g, Percentage of cercariae (~50) continuing to swim over three minutes after addition of each compound at specified final concentrations. Triplicates were performed. Data are mean ± S.D.

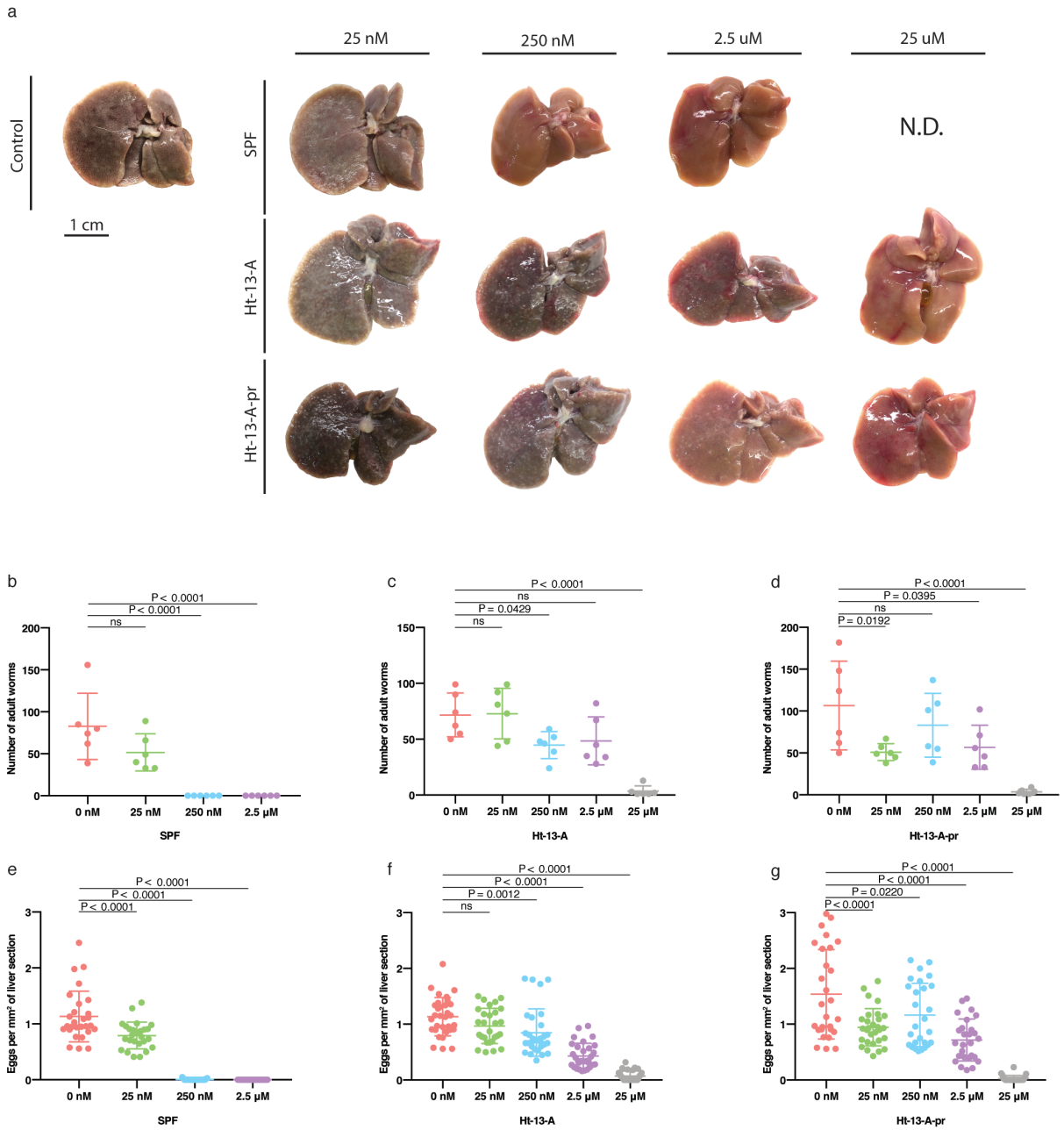

Figure 4 | Treating cercariae with SPF, Ht-13-A or Ht-13-A-pr blocks schistosome infection and alleviates pathology. a, Representative livers (post perfusion) from mice (N=6) infected with drug-treated cercariae. Livers from mice treated with control and lower drug concentrations were darker in color and contained more granulomas (white spots). With higher drug concentrations, livers had normal morphologies with few or no granulomas. 25 μM SPF treatment was not determined (N.D.) due to limited amounts of purified SPF. **b-d,** Numbers of adult worms recovered from infected mice (two experiments for each drug, 6 mice total for each condition). **e-g,** Numbers of schistosome eggs per area (/mm^2) from liver sections (4-6 sections per mouse). Data (**b-g**) are mean ± S.D. Statistics: One-way ANOVA, post Dunnett's test.